

Extended, monolayer flat islands and exciton dynamics in $\text{Ga}_{0.47}\text{In}_{0.53}\text{As}/\text{InP}$ quantum-well structures

X. Liu* and S. Nilsson†

Department of Solid State Physics, Lund University, Box 118, 22100 Lund, Sweden

L. Samuelson

*Department of Solid State Physics, Lund University, Box 118, 22100 Lund, Sweden
and Departamento de Física, Pontifícia Universidade Católica do Rio de Janeiro, Rio de Janeiro, Brazil*

W. Seifert

*Department of Solid State Physics, Lund University, Box 118, 22100 Lund, Sweden
and Epiquip AB, S-223 70 Lund, Sweden*

P. L. Souza

*Department of Solid State Physics, Lund University, Box 118, 22100 Lund, Sweden
and Centro de Estudos em Telecomunicacoes, Pontifícia Universidade Católica do Rio de Janeiro, Rio de Janeiro, Brazil*

(Received 13 July 1992)

Spectroscopic studies are performed on multiple-quantum-well structures of $\text{Ga}_{0.47}\text{In}_{0.53}\text{As}/\text{InP}$ grown by low-pressure, metal-organic vapor-phase epitaxy. The compositional gradient and thickness variation at interfaces are probed by exciton recombination in the quantum wells. Spectral and topological observations of extended, monolayer flat islands are demonstrated by photoluminescence and cathodoluminescence. Different exciton transfer mechanisms are studied by the temperature-dependent, photoluminescence spectroscopy of these quantum-well structures. Depending on the temperature, in addition to exciton localization in the extended monolayer flat islands, exciton migration within the quantum well, i.e., intralayer (lateral) transfer, occurs as well as thermal detrapping to the InP barrier and subsequent recapture into neighboring, thicker quantum wells, i.e., interlayer (perpendicular) transfer. Rates for carrier capture into quantum wells in the ps range are extracted from the temperature dependence of quenching processes of photoluminescence. Quantitative analysis of exciton migration is carried out based on absorption measurements. The results show that, due to exciton migration, attempts to estimate the area ratio of monolayer islands of different thicknesses by luminescence intensities result in a severely distorted picture, with the area of thicker islands being greatly overestimated.

I. INTRODUCTION

Structural and chemical interface imperfections in the form of compositional gradients and morphological fluctuations have a strong influence on the electronic and optical properties, and thus are limiting factors in the performance, of devices based on semiconductor heterostructures.^{1,2} Great effort has been devoted to the development of epitaxial-growth techniques which are able to satisfy the stringent requirements of structural smoothness and chemical abruptness at heterointerfaces. The best-adapted growth techniques so far are molecular-beam epitaxy (MBE), metal-organic vapor-phase epitaxy (MOVPE), and chemical beam epitaxy. With these techniques and a sophisticated set of options for characterization and control of the growth, it has now become possible to deposit ultrathin layers with thicknesses of only a few atomic layers and with heterointerfaces which are abrupt to within about one atomic monolayer, a result which has been attributed to a two-dimensional, layer-by-layer growth mechanism.³⁻⁹ The procedure of growth interruption at either one or both heterointerfaces is widely applied in both MBE and MOVPE growth to

improve the interface smoothness.⁹⁻¹³ When growth is interrupted before the deposition of a succeeding layer, the density of atomic-scale, morphological roughness is expected to diminish as the smaller growth islands relax into larger ones due to the migration of the lattice constituents to steps where they are incorporated. With increasing interruption, two other effects must be considered, namely (i) exchange processes between the interrupted surface and the ambient environment and (ii) the deposition of impurities on the exposed surface. The formation of growth islands with a lateral extent much larger than the free-exciton Bohr diameter, called extended monolayer flat islands, has been reported for $\text{GaAs}/\text{Al}_{1-x}\text{Ga}_x\text{As}$ as well as for $\text{Ga}_{1-x}\text{In}_x\text{As(P)}/\text{InP}$ quantum-well heterostructure systems.¹²⁻¹⁷

Several different techniques have been used to characterize the heterointerface quality.¹⁸⁻²¹ In particular, luminescence spectroscopy is widely used to provide information about the morphological roughness (sometimes the compositional gradient) of quantum-well (QW) structures.²² Regarding the morphological roughness, when a large number of growth islands smaller than the free-exciton Bohr diameter, called microroughness, occurs at

the heterointerface, it is considered that the induced, random, potential fluctuations are averaged over the exciton wave function. From such a heterointerface configuration, the luminescence peak would be broadened around the energy position corresponding to the mean quantum-well thickness.²³ When improvements of the growth conditions lead to the formation of extended, monolayer flat islands, the excitons can be considered as being confined in areas of discrete quantum-well thickness. "Monolayer splitting" in the luminescence spectrum is thus expected for such a heterointerface configuration, in which the energy of the individual peaks of the multiplet corresponds to a quantum well whose thickness is multiples of one monolayer.⁹ However, transients in compositions may still occur which cannot be easily detected by photoluminescence (PL) on only one sample.²¹

Already in the case of a heterointerface with microroughness, and in the more recent case of extended, monolayer-smooth heterointerfaces, many different phenomena related to exciton dynamics have been investigated.²⁴⁻³¹ It has been found that intralayer communication by diffusion may be limited at the lowest temperatures due to hampered migration. At higher temperatures, intrawell thermalization across the boarder surrounding flat islands can be expected, and for sufficiently high temperatures, thermal emission out of quantum wells is expected to result in quenching of the luminescence intensity. Since luminescence spectra reflect radiative recombination of carriers which have already thermalized, it is very difficult to get information about the relative areas of islands of different thickness in a QW. A quantitative method, such as absorption spectroscopy, is therefore important in order to gain such information.

In this study, multiple-quantum-well structures of $\text{Ga}_{0.47}\text{In}_{0.53}\text{As}/\text{InP}$, grown by MOVPE employing growth interruption, are investigated by absorption, PL, and cathodoluminescence (CL) spectroscopies. The investigation is focused on the spatial and temperature variations of the excitonic transition processes. Observations of extended islands with almost monolayer flat interfaces are presented. The processes governing the temperature dependence of the luminescence intensity are identified in terms of intralayer and interlayer transfer processes, with different types of exciton dynamics dominating different temperature regions. From the thermal quenching of the luminescence occurring at higher temperatures, time constants have been estimated for carrier capture into quantum wells occurring on the ps scale. Furthermore, from the quantitative analysis of exciton migration based on absorption and luminescence measurements, conclusions are drawn that exciton transfer is significant even at the lowest temperature, and attempts to estimate the areas of monolayer flat islands from luminescence spectra will result in a severely distorted picture, with the area of thicker islands being greatly overestimated.

II. EXPERIMENT

This study was performed on lattice-matched, $\text{Ga}_{0.47}\text{In}_{0.53}\text{As}/\text{InP}$ multiple-quantum-well structures pri-

marily on two samples grown by MOVPE on Sn-doped, [100]-oriented InP substrates (Sumitomo), with a misorientation of less than $\pm 0.5^\circ$. A comprehensive description of the MOVPE system is given in Ref. 17. Briefly, the MOVPE growth of the samples was carried out in a horizontal reactor at 600 °C, and at reduced pressure, 50 mbar, using trimethylindium (TMIn), trimethylgallium (TMGa), arsine (AsH_3), and phosphine (PH_3) as precursors. The doping level in the nominally undoped material is $n \approx 1 \times 10^{15} \text{ cm}^{-3}$. Gas switching was done between pressure- and flow-balanced reactor and vent lines with a fast switching manifold of approximately 0.1-s response time, designed with a negligible dead volume. In addition, a high gas velocity (2.73 m / s) was used to further ensure the fast switching of the composition of the growth species. To improve the interface abruptness, growth interruption was employed at both interfaces of each quantum well. The switching sequences used for the two samples, EQ72 and EQ99, are illustrated schematically in Table I. The growth was interrupted for 2 s with no group-III flow and the group-V gases were changed in the middle of the interruption time either instantly or with a delay time of 1 s. Table I also summarizes the principal growth parameters and the growth times for each $\text{Ga}_{0.47}\text{In}_{0.53}\text{As}$ layer. Consequently, the two samples contain a 250-nm InP buffer layer, followed by a sequence of $\text{Ga}_{0.47}\text{In}_{0.53}\text{As}$ quantum wells, with quantum-well widths associated with the growth times shown in the last column of Table I. The quantum wells were separated by InP spacer layers which are sufficiently wide, 20 nm, for tunneling effects to be insignificant. The epitaxial growth was completed by the deposition of 35-nm InP as a capping layer. In sample EQ72 a bulk $\text{Ga}_{0.47}\text{In}_{0.53}\text{As}$ reference layer was grown before the quantum-well structures were deposited, with the use of the same set of parameters as that for the quantum wells, from which the composition of $\text{Ga}_{1-x}\text{In}_x\text{As}$ was monitored.

CL, PL, and absorption measurements were employed for the characterization of the quantum-well structures. The CL measurements were performed using a scanning electron microscope operating at 10 keV, modified with a CL collector and a continuous helium-flow stage cooled to about 25 K. The technique has previously been described in detail.³² The current of the electron beam hitting the samples was about 10 nA. The emission from the sample was dispersed by a 0.50-m monochromator (30-Å bandpass) and detected by a nitrogen-cooled germanium photodiode in conjunction with conventional lock-in techniques utilized by chopping the electron beam. Because the diffusion of electron-hole pairs falls rapidly from the generation volume, spatial resolution of the CL system could be estimated from the electron energy loss along the electron trajectory in the solid, i.e., from the generation volume.³³ Monte Carlo simulation computations applied to bulk $\text{In}_{1-x}\text{Ga}_x\text{As}$ give a generation volume of 1.0 μm in diameter for an incident electron beam energy of 10 keV.

PL was excited above the InP energy gap using the 514.5-nm emission line from an Ar^+ laser. The sample temperatures were varied from 2 to 450 K. A combi-

TABLE I. Growth parameters, growth schedules, and structures of the samples. SCCM denotes cubic centimeter per minute at STP.

Sample	T_G (°C)	H_2 (SCCM)	AsH_3 (10^{-5} mole fraction)	PH_3	TMGa	TMIn	Growth Schedules								Growth Sequences of Quantum Wells (s)
							0	2	4	6	8	10	12	14	
EQ72	600	5800	124	674	0.58	0.69	In ————								Ref-20-10-5-3-2-1
							Ga ————								
							PH ₃ ————								
							AsH ₃ ————								
EQ99	600	5800	50	1900	0.56	0.66	In ————								6 - 6 - 6 - 6
							Ga ————								
							PH ₃ ————								
							AsH ₃ ————								

cryostat, with the samples either immersed in liquid helium or cooled in a helium-vapor flow at a controlled temperature, was used up to room temperature. At higher temperatures, the samples were mounted on an electrically heated sample holder. The typical excitation power on the sample was about 10^2 W / cm^2 . The PL was dispersed by a double-grating, 0.75-m monochromator. A nitrogen-cooled germanium photodiode was used with lock-in detection.

Absorption measurements were carried out by measuring the transmission of a reference InP sample and the QW structure. The absorption spectra are obtained by dividing the transmission spectrum of the former by the latter. The experimental setup is very similar to that of PL, except that the sample is illuminated by a tungsten lamp, and a silicon photodiode is used for detection.

III. RESULTS AND DISCUSSION

A. Probing the interfaces of QW's by excitons

At interfaces of the $Ga_{0.47}In_{0.53}As/InP$ QW's, the compositional gradient along the growth direction occurs, as well as the thickness variation in the QW plane. The two-dimensional character of the growth makes it possible to discuss QW's in terms of a thickness of a certain number of monolayers even when composition transients are present on one or both of the QW interfaces.

Presented in Fig. 1 are typical 2-K PL spectra of one of the investigated $Ga_{0.47}In_{0.53}As/InP$ multiple-quantum-well structures, EQ72, containing nominally six quantum wells of various thicknesses, corresponding to the growth times listed in the last column of Table I. As can be seen, the PL spectrum consists of luminescence peaks which are split into multiplets, corresponding to exciton recombinations in QW's with thicknesses of multiples of one atomic monolayer ($1ML \approx 2.93\text{\AA}$). Doublets, instead of triplets, are observed for the luminescence from a QW, implying that the two interfaces of the QW are inequivalent, with perhaps the binary compound (InP) surface smooth more rapidly during growth than the ternary compound (GaInAs) surface does, similar to the case of $Al_{1-x}Ga_xAs/GaAs$ structures.²² This picture of the interface is consistent with the observation of high-resolution transmission electron microscopy in Fig. 2,

and will be further discussed below. In the spectral region of the thinnest quantum wells (corresponding to the growth times of 1, 2, and 3 s), however, broad features between peaks of multiples of 1 ML are observed. The origin of these features is not yet clear and is still under investigation. In the present study, we focus on the luminescence due to exciton recombinations in QW's with thicknesses of multiples of 1 ML.

For the $Ga_{0.47}In_{0.53}As$ multiple-quantum-well structures studied, it is believed that low-temperature luminescence is due to free-exciton recombination as evidenced by the narrow full width at half maximum (FWHM) and the linear dependence of intensity on excitation power for the PL emission peaks associated with the quantum wells. In fact, except for the results from chemical beam epitaxial $Ga_{1-x}In_xAs$ single quantum wells, which exhibit the narrowest FWHM ever observed, the FWHM in our samples are about as small, or smaller than, the best reported line widths. The FWHM of the 2-K PL peaks were approximately 8.0 meV for the emission peak of the

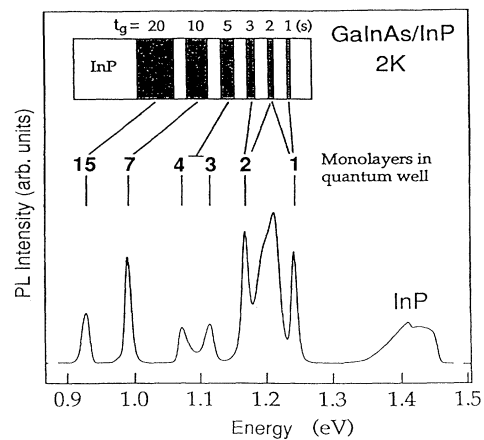


FIG. 1. Photoluminescence spectra at 2 K of the investigated $Ga_{0.47}In_{0.53}As/InP$ multiple-quantum-well structure, sample EQ72. For each nominal quantum well grown according to the growth sequence, the spectra consist of PL emission lines which are split into multiplets. The sample structure and the thickness of the quantum well corresponding to each of the luminescence lines are shown in the inset.

quantum well with a growth time of 1 s, which is believed to correspond to a quantum-well thickness of nominally 1-ML $\text{Ga}_{0.47}\text{In}_{0.53}\text{As}$.¹⁷

1. Vertical gradient in composition

The growth rates of an $\text{Ga}_{0.47}\text{In}_{0.53}\text{As}$ quantum well and an InP barrier can be estimated from the macroscopic growth rate for the respective thick layers, which are confirmed by studies on the sample EQ99 by transmission electron microscopy (TEM). As illustrated in Table I,

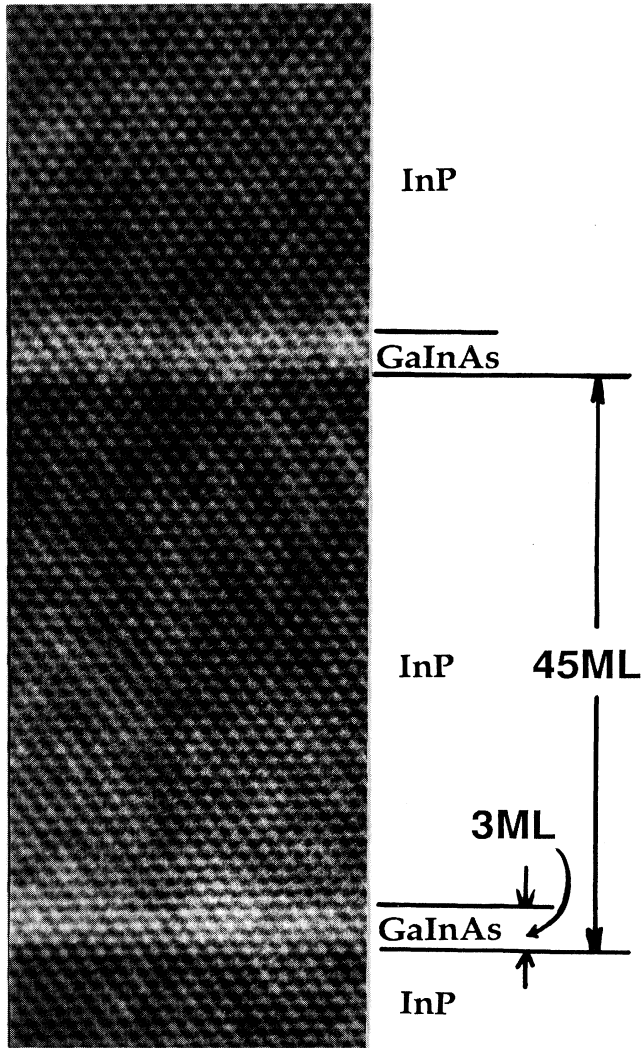


FIG. 2. Micrograph of $\text{Ga}_{0.47}\text{In}_{0.53}\text{As}/\text{InP}$ multiple-QW structures (sample EQ99) obtained from high-resolution transmission electron microscopy. It shows a sharp lower $\text{InP}/\text{Ga}_{0.47}\text{In}_{0.53}\text{As}$ interface and a more diffuse upper $\text{Ga}_{0.47}\text{In}_{0.53}\text{As}/\text{InP}$ interface. The exact thickness of the $\text{Ga}_{0.47}\text{In}_{0.53}\text{As}$ well is thus hard to determine. However, one can obtain a more accurate value of 45 ML for the thickness between two sharp interfaces, i.e., the thickness of the InP barrier plus the $\text{Ga}_{0.47}\text{In}_{0.53}\text{As}$ well. Taking into account the growth time of 3 min for the InP barrier and 6 s for the $\text{Ga}_{0.47}\text{In}_{0.53}\text{As}$ well, the thickness of the $\text{Ga}_{0.47}\text{In}_{0.53}\text{As}$ well can then be determined to be 3 ML.

sample EQ99 contains a stack of 10 QW's, each of them grown for 6 s. On a sample position where a growth rate of 0.5 ML/s is expected, the TEM picture is presented in Fig. 2. It shows a sharp, lower $\text{InP}/\text{Ga}_{0.47}\text{In}_{0.53}\text{As}$ interface and a more diffuse, upper $\text{Ga}_{0.47}\text{In}_{0.53}\text{As}/\text{InP}$ interface, in accordance with the earlier observations of Carey *et al.*³⁴ Due to this diffusivity at the upper interface, the exact thickness is difficult to determine, but it is between 4 and 5 ML. On the other hand, a more accurate value can be calculated by the observation that the distance between two sharp interfaces, i.e., the thickness of the InP barrier plus the $\text{Ga}_{0.47}\text{In}_{0.53}\text{As}$ well, is exactly 45 ML. It is therefore calculated that the "thickness" of the $\text{Ga}_{0.47}\text{In}_{0.53}\text{As}$ well is 3 ML, taking into consideration that the growth rate for InP is about half that of $\text{Ga}_{0.47}\text{In}_{0.53}\text{As}$ and the growth time is 3 min for the barrier and 6 s for the well. The "growth rate" is thus 0.5 ML/s for the $\text{Ga}_{0.47}\text{In}_{0.53}\text{As}$ well and 0.25 ML/s for the InP barrier, in agreement with the respective macroscopic growth rate.

The term "thickness" used above, however, is not clearly defined. It is known, however, that attempts to make extremely abrupt transitions during the growth lead to complicated interfaces resulting from various surface interactions.^{35–38} The additional 1–2 ML in thickness seen in the TEM picture is believed to be due to the $\text{InAs}_x\text{P}_{1-x}$ interface layer formed by the interaction of AsH_3 with the barrier material at the lower interface and a carryover of arsenic into the InP at the upper interface. Recently it is found that the AsH_3 pressure is a very critical parameter.³⁹ Thus the thickness above refers to the "nominal thickness" of the true $\text{Ga}_{0.47}\text{In}_{0.53}\text{As}$ well material. The "effective potential" of the QW, however, is determined by its "effective thickness" which is the total thickness including interface layers, namely the sum of the thicknesses of lower interface $\text{InAs}_x\text{P}_{1-x} + \text{Ga}_{0.47}\text{In}_{0.53}\text{As}$ plus upper interface $\text{InAs}_y\text{P}_{1-y}$. Obviously, the luminescence energy of two QW's with the same nominal thickness of $\text{Ga}_{0.47}\text{In}_{0.53}\text{As}$ material can be different depending on the interfaces which vary as a function of growth conditions, especially the growth interruption sequences and the AsH_3 pressure. For the two samples investigated, EQ72 and EQ99, different growth interruption sequences were used during their fabrication, as illustrated in Table I. A weaker AsH_3 interaction with the lower InP barrier material is expected in sample EQ99, since there was an interruption time of 1 s without AsH_3 and its flow started together with the TMG and TMI for the well growth. In sample EQ72, however, a strong substitution of P by As in the barrier material is expected, since the AsH_3 flow was started 1 s before the growth of the QW's. Consequently, a shift of the luminescence energy from a QW in sample EQ72 toward a longer wavelength is expected in comparison with that from a QW in EQ99 with the same nominal thickness. This shift is indeed observed (compare Figs. 1 and 11).

The nominal thicknesses of the QW's corresponding to each of the luminescence peaks are indicated in the inset in Fig. 1 for sample EQ72. This assignment is both in agreement with the macroscopic growth rate of 0.7 ML/s

expected for the sample position where the PL spectrum in Fig. 1 is taken, and in agreement with our detailed growth investigation in the thinnest QW region reported recently.³⁹ It is also consistent with the confined energy levels of electrons and heavy holes theoretically calculated by taking into account the $\text{InAs}_x\text{P}_{1-x}$ interface layers and modeling the effective potentials of such a QW. The detailed theoretical treatment is beyond the scope of the present study and will be presented elsewhere.

2. Lateral variation in thickness

In a number of earlier publications, PL spectra similar to that in Fig. 1 for sample EQ72, containing doublet or triplet emission lines, have been attributed to free-exciton recombination from areas differing by one monolayer in width within one quantum well.²² Since well-defined excitonic emission lines are observed, the monolayer flat islands must be larger in lateral extension than the Bohr diameter of the free exciton (extended monolayer flat islands). A CL imaging investigation performed on sample EQ72 seems to have provided further support for the presence of atomically flat interfaces.⁴⁰ It was shown that spectrally resolved CL images formed for the individual CL emission peaks in a multiplet resulted in images which were highly complementary in contrast. Based on this result, the CL images were interpreted as directly reflecting the dimensions over which monolayer flat islands occur. The upper boundary of the lateral extent was determined to be $\approx 2 \mu\text{m}$. However, the validity of this interpretation of CL images will be further discussed below, leading to a need for reinterpretations.

Resulting from the growth mode which produces extended, almost monolayer flat islands, a discontinuous energy shift of the PL peaks is expected upon changing the growth time per quantum well, since the width of a quantum well can be changed only in multiples of 1 ML. Thus, upon increasing the growth time per quantum well an increase of the areas of the wider quantum well should manifest itself as a shift of the luminescence intensity from higher to lower energy peaks. For a further increase in growth time, an additional luminescence peak at a lower energy should appear. In a recent study, this kind of experiment has been performed on the $\text{Ga}_{0.47}\text{In}_{0.53}\text{As}/\text{InP}$ quantum-well system and it has been shown that a discontinuous energy shift of the luminescence emission lines is obtained for quantum wells with nominal widths from 1–8 ML when the growth time per quantum well is varied.⁹ The growth conditions used in that study should favor a two-dimensional mode of growth, i.e., the growth takes place monolayer by monolayer and the growth of an additional monolayer starts when a two-dimensional nucleus has been formed on the surface.

In the current study a similar experiment was carried out. However, the samples studied here were grown without the use of sample rotation, since this technique has been found to yield the sharpest interfaces. Hence, the growth rate varies across the wafer and the variation of the energy and intensity of the luminescence emission was investigated for the $\text{Ga}_{0.47}\text{In}_{0.53}\text{As}/\text{InP}$ multiple-quantum-well structure. A CL line scan was recorded at

positions with equidistant shifts of $500 \mu\text{m}$ along a distance of 15 mm across the sample. A sample temperature of 25 K was chosen, which is the lowest temperature achievable in our CL system.

The presence of extended, monolayer flat islands in our sample is evidenced by the observation in Fig. 3 which displays the evolution of the multiplet spectra, arising from the quantum wells with 5- and 10-s growth times of sample EQ72. It is readily seen that in going from the lower to the upper spectra in the figure, the CL intensity shifts toward peaks of the lower energies in the respective multiplet, and as the spectra evolve across the sample, peaks appear on the low-energy side of the multiplet. In Fig. 4, the emission energies corresponding to the different peaks of Fig. 3 are presented. Only CL peaks at distinct energies are observed. For each of the emission energies the variation is less than 5 meV, while the monolayer splitting is typically 50 meV, depending on the thicknesses of the QW.

The occurrence of multiplets in the luminescence spectra is caused by areas of different widths in the same quantum well, and the appearance of a peak on the low-energy side of the multiplet marks the beginning of the growth of the next monolayer. Thus the growth rate is reflected in the evolution of the multiplets where a set of points across the sample corresponds to a lateral varia-

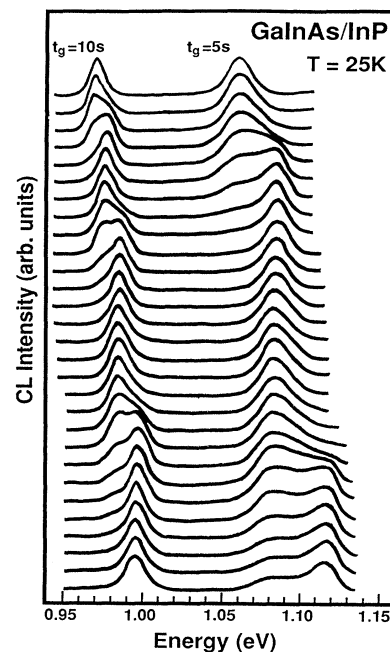


FIG. 3. Cathodoluminescence spectra of sample EQ72 at a temperature of 25 K, showing the evolution of two multiplets as a function of position across the sample. The two multiplets arise from the quantum wells for growth times of 10 and 5 s, respectively. Due to a decreasing growth rate from the top to the bottom spectra, a discontinuous shift of the CL peaks to the higher energies resulting from recombinations of excitons confined in 1-ML thinner quantum wells is clearly observed. Note that the intensity of each spectrum has been normalized to the most intense peak in the multiplet.

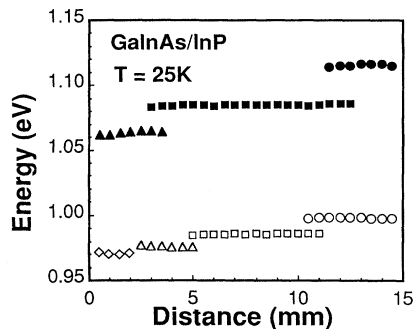


FIG. 4. Cathodoluminescence emission energies at 25 K as a function of position across the sample, corresponding to the different CL peaks in Fig. 3 for sample EQ72.

tion of the growth rate. It is expected that compositional gradient would not depend on the growth rate of the quantum well (i.e., on the thickness of the quantum well). However, the areas of islands of different thicknesses should depend on the exact amount of material used for the growth of the quantum well, namely on the growth time. This is demonstrated in Fig. 3, which shows that as one CL peak appears and disappears in the evolution of the multiplet for the quantum well with the growth time of 5 s, two peaks are observed to vary for the quantum

well with a growth time twice as long (i.e., 10 s). Hence, although the growth rate varies laterally across the sample, as revealed by the evolution of the multiplets along the CL line scan, the growth rate remains almost the same in the direction of the growth for a fixed position on the sample.

B. Exciton dynamics in quantum-well structures

Exciton recombinations in our high-quality samples provide a unique opportunity for investigating exciton dynamics in quantum-well structures. In this section, temperature-dependent PL studies are presented which offer a convenient way to investigate the migration of the free excitons (free carriers) in terms of lateral transfer within a quantum well (intralayer transport), and perpendicular transfer between different neighboring quantum wells (interlayer transport).³¹ The results presented in this section are primary on sample EQ72.

The microscopic fluctuations in width of a QW can be regarded as perturbations which affect the line shape of excitons in emission spectra. As the sizes of the interface defects increase and become large in comparison with the Bohr diameter of the exciton, it becomes more reasonable to assume that each quantum well is composed of several areas of different widths.²³ As a consequence of increased spatial coherence of the excitonic states, separated exci-

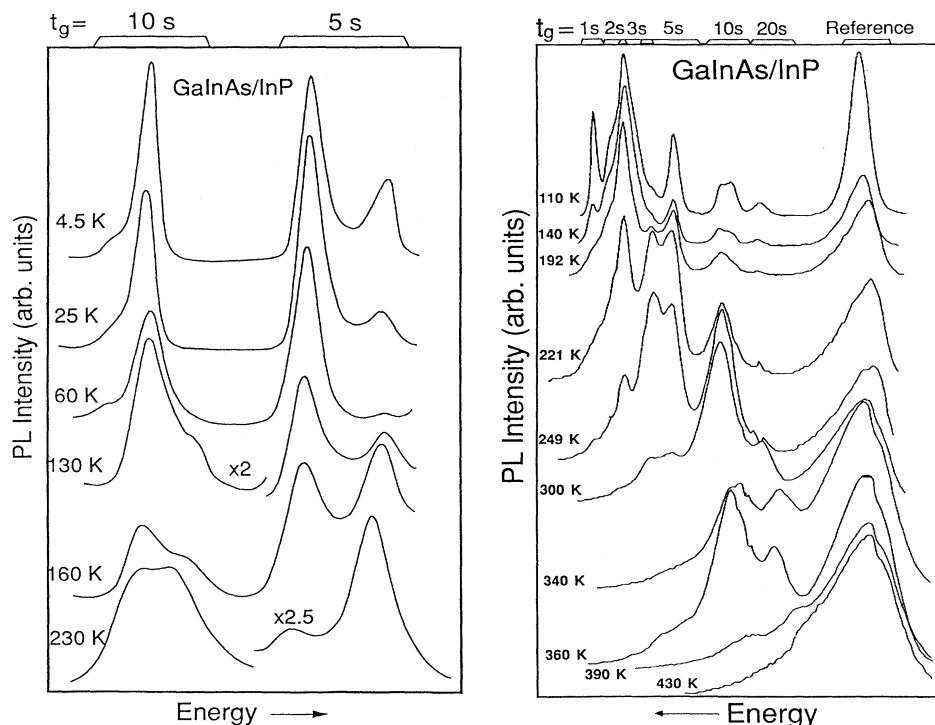


FIG. 5. Photoluminescence spectra of the $\text{Ga}_{0.47}\text{In}_{0.53}\text{As}/\text{InP}$ multiple-quantum-well structure (sample EQ72) measured at different temperatures between 1.5 K and 450 K. The spectra are shown in two series: (a) those from quantum wells for the growth times of 10 and 5 s intended for the illustration of intrawell transfer at lower temperatures and (b) those from all the six quantum wells intended for the illustration of interwell transfer at higher temperatures. The growth times of the nominal quantum wells are displayed on the upper abscissa and assigned to their respective multiplet peaks. Note that spectra in (a) and (b) correspond to different excitation positions on the sample. The PL intensities are adjusted for comparable heights. The spectra at different temperatures are shifted in energy to align the peaks.

tonic transitions with narrower linewidths are observed (as in the high-quality samples currently being investigated). This provides a unique opportunity for studying the transfer of excitons between different, extended, quantum-well islands.

Most of the (minority) carriers generated in the InP layers were assumed to be trapped in the quantum wells by fast diffusion and capture processes. Nonradiative or radiative recombination in the barriers do not significantly lower the carrier collection efficiency of the quantum well because the transfer time is certainly orders of magnitude shorter than typical nonradiative and radiative lifetimes in nominally undoped InP.⁴¹

Temperature dependences of the PL up to 450 K are studied, in order to observe a complete thermal quenching of all the PL peaks arising from the multiple-QW structure. Figure 5 shows typical temperature-dependent PL spectra with Figs. 5(a) and 5(b) intended to demonstrate the exciton dynamics of intrawell and interwell transfer, respectively [note that Figs. 5(a) and 5(b) are recorded at different sample positions, and correspond to different temperature ranges]. For each of the PL multiplets arising from the six nominal quantum wells, the evolution of the luminescence intensity is observed to be altered in a regular way as the temperature is increased, and their temperature dependence can be divided into four characteristic temperature regions. The results of Fig. 5 are summarized in Fig. 6 for the temperature dependence of the integrated intensity of the PL peaks corresponding to the quantum well with thicknesses of 3

and 4 ML grown for 5 s, and the quantum well with a thickness of 2 ML grown for 3 s. The temperature dependence is qualitatively interpreted in terms of different exciton dynamics which are predominant in different temperature ranges.

1. Localization or trapping

In *temperature range I*, the PL intensity is almost constant. This is believed to be due to less mobile excitons at the lowest temperatures, following the capture into the quantum well of the photogenerated carriers in the InP barriers. In this temperature region, even very small potential fluctuations in the quantum well are sufficient to trap excitons (process α in the inset of Fig. 6). Such potential fluctuation could arise either from (i) fluctuations in alloy composition, (ii) fluctuations, on an atomic scale, in the width of the quantum well, or (iii) local potential maxima occurring along the periphery of the islands. This localization of excitons limits the intrawell transfer to the 1-ML thicker, low-energy regions of the quantum well. This is in excellent agreement with the PL study of very thin $\text{Ga}_{1-x}\text{In}_x\text{As}/\text{InP}$ quantum wells reported in Ref. 41. The interpretation given in that paper is that the luminescence at 10 K and at low excitation densities is due to localized exciton recombination, while at temperatures above 10 K and at higher excitation densities, exciton delocalization is observed.

If the excitons are 100% trapped in this temperature region, the luminescence intensities from islands of different thicknesses in a quantum well should directly reflect the areas of the islands. However, as will be discussed in Sec. III D, this is not the case. It is true that the exciton migration is hampered by small potential fluctuations in the quantum well, but the exciton transfer, which does not have to overcome any potential barrier, still plays an important role in the exciton dynamics, even in the lowest temperature region.

2. "Down-hill" migration

In *temperature range II*, at slightly higher temperatures, the PL intensity from regions of 4 ML increases at the expense of that from the 3-ML regions. In this temperature range, the delocalization of excitons quenches the luminescence from the narrow regions of the quantum well because the excitons are further thermally activated and migrate into the regions of lower confinement energy, corresponding to thicker quantum-well regions. Hence, an intralayer exciton transfer from 3-ML regions to 4-ML regions takes place (process β in the inset of Fig. 6). In this temperature range, the relative PL intensities are basically determined by the competition between the radiative recombination lifetime within the terrace and the exciton transfer (drift) time to the neighboring island regions with well widths 1-ML thicker. The result, as the temperature increases, that the PL intensity from the 3-ML regions decreases and almost vanishes at 45 K, suggests that the exciton transfer time from 3- to 4-ML regions is much shorter than the radiative lifetime (at the current temperature).

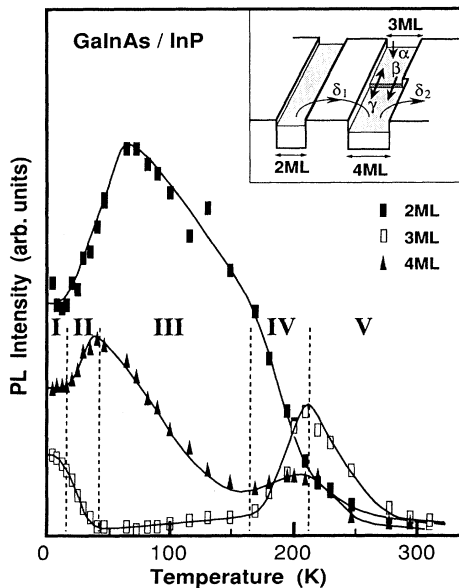


FIG. 6. Temperature dependences of the integrated photoluminescence intensities originating from quantum wells with thicknesses of 2, 3, and 4 ML in sample EQ72. The solid lines are guide lines for the eye. The inset shows schematically the different exciton transfer mechanisms: localization (α), down-hill migration (β), up-hill thermalization (γ), and interwell capture (δ_1) and emission (δ_2) which dominate in different temperature ranges: I, II, III, IV, and V, respectively.

It should be pointed out in this connection that the existence of a “down-hill” migration process in fact suggests the existence of an exciton-trapping process at lower temperatures. Otherwise, with increasing temperature, the only intrawell exciton dynamics observed should probably be the “up-hill” thermalization to be discussed next.

3. ‘Up-hill’ thermalization

In *temperature range III*, the variation of the PL intensity is characterized by a decrease in the intensity from the 4-ML regions and an increase of the intensity from the 3-ML regions. This is the result of the thermal equilibrium of neighboring regions differing in thickness by 1 ML (intrawell thermalization, process γ in the inset of Fig. 6). When the thermal energy of the exciton exceeds the potential step, i.e., the energy barrier due to fluctuation of 1 ML in the quantum-well width, excitons can be thermally excited into the narrower quantum-well regions. This thermalization process (the Boltzmann thermalization) can be verified by the analysis of the ratio between the intensities [$I_{3\text{ML}}/I_{4\text{ML}}$] studied as a function of temperature.

$$I_{3\text{ML}}/I_{4\text{ML}} = (S_{3\text{ML}}/S_{4\text{ML}}) \exp(-\Delta E_{34}/kT), \quad (1)$$

where $S_{3\text{ML}}/S_{4\text{ML}}$ is the ratio of the density of state of the 3- and 4-ML exciton bands, which should be proportional to the ratios of the island areas, and ΔE_{34} is the potential step of the 3- and 4-ML excitonic states. The Arrhenius plot is shown in Fig. 7, based on the data in Fig. 6. A single activation energy of about 42 meV is obtained in this temperature region, which is very close to the intra-quantum-well potential step experienced by the exciton, 45 meV, as deduced from the difference in PL energies between the transitions of the two confined states arising from quantum wells with thicknesses of 3 and 4 ML. This result may imply that the exciton moves

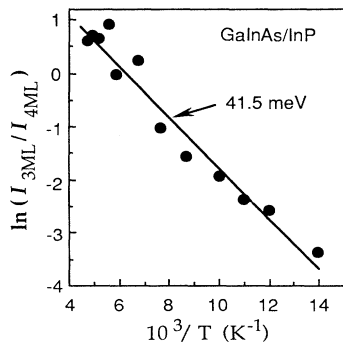


FIG. 7. Temperature dependence of the integrated photoluminescence intensity ratio for sample EQ72: $I_{3\text{ML}}/I_{4\text{ML}}$ shown on an Arrhenius plot, where $I_{3\text{ML}}$ and $I_{4\text{ML}}$ are the photoluminescence intensities arising from the three-monolayer regions and the four-monolayer regions within the quantum well, respectively. The thermal activation energy is determined to be about 42 meV. Extrapolation of the plot to infinite temperature allows an estimation of the ratio of three- and four-monolayer areas, which gives a result of $S_{3\text{ML}}/S_{4\text{ML}} = 20$.

laterally in a quantum well as a single entity.

Equation (1) and Fig. 7 allow us to estimate the ratio between the areas of the islands of 3 and 4 ML thickness. By extrapolating Fig. 7 to infinite temperature, the area ratio of 3- and 4-ML islands is obtained as: $S_{3\text{ML}}/S_{4\text{ML}} \approx 20$. This result is very surprising, since it means that even though the luminescence intensities from 3- and 4-ML islands are similar for this sample position at low temperature, the area of the 3-ML islands is much larger than that of the 4-ML islands. This, however, is in good agreement with the results of absorption measurements performed on sample EQ99, which was grown for absorption measurements in order to determine the relative island areas. As will be presented in Sec. III D, the luminescence intensity of the lower energy peak in a multiplet may be much stronger than that of the higher energy peak, even though the absorption at the higher energy peak is stronger.

In this temperature range, it is also noted that the total integrated PL intensity from the quantum well (for the growth time of 5 s) decreases with increasing temperature. This decrease in intensity is believed to be caused by temperature-activated nonradiative processes in the quantum well. This corroborates the results of Ref. 41, where, for a $\text{Ga}_{1-x}\text{In}_x\text{As}/\text{InP}$ quantum well, a strong nonradiative recombination was observed at temperatures above 40 K.

4. QW luminescence quenching due to thermal emission processes

In *temperature range IV*, at higher temperatures, an increase of the PL intensity is observed from both 3- and 4-ML regions, corresponding to 5-s growth time, and simultaneously, a significant decrease in the PL intensity from the thinner quantum well, with growth time of 3 s. Any temperature-dependent tunneling processes through the barriers seems unlikely due to the large thicknesses of the barriers, about 20 nm. Instead, it is concluded that the behavior is due to a thermal detrapping of excitons from the thinner well to the InP confining barrier and the subsequent recapture and recombination in the thicker quantum well (process δ_1 in the inset of Fig. 6).

In *temperature range V*, at further increased temperatures, the PL intensity decreases from both the 3- and 4-ML regions (for growth time of 5 s). The behavior is attributed to the same detrapping mechanism as is observed in temperature range IV. In this temperature region, thermal detrapping from the quantum well with 3 and 4 ML to the InP barriers starts and becomes dominant (process δ_2 in the inset of Fig. 6). Similarly, a simultaneous increase in the PL intensity from an even thicker quantum well (for growth time of 10 s) is observed [see Fig. 5(b) for an overview].

The trend observable in Fig. 5(b) implies that the effect of this loss by thermally activated detrapping to the barriers is reduced or eliminated by increasing the quantum-well thickness, or conversely, by increasing the barrier height. There is a continuous shift in the critical temperature of quenching in going to thicker and thicker QW's, corresponding to an increase in the activation en-

ergy from the ground state to the barrier. For instance, the temperature for which quenching starts varies from 125 K for the thinnest QW up to 375 K for the thick reference layer. In Sec. III C below, this trend will be analyzed, and it will be shown that detailed balance between emission out of and capture into a QW can give information on the very fast processes by which carriers are captured into QW's.

C. Exciton emission and capture processes in quantum-well structures

An important question is whether the detrapping mechanism is the emission of an exciton as a single entity or whether one has to consider separately the loss of electrons and holes from the QW. Accurate determination of the activation energies of quenching processes are complicated by the interference in our multiple QW structures from intrawell and interwell transfer processes, etc. On the other hand, much effort has been devoted to determining the kinetics of the inverse process, i.e., measuring the ultrafast (\approx ps) time constants for the capture of carriers and excitons into quantum wells.⁴² In this section a method is proposed to estimate these fast capture time constants using the well-width dependence of the PL quenching process for sample EQ72 as in Fig. 5(b).

With increasing temperature the radiative recombination will eventually be quenched as carriers are emitted out of the quantum well at a rate faster than the intrawell recombination rate. For the temperature T' at which a kink in the plot of PL intensity versus temperature occurs, namely the onset of the quenching process, it is assumed that carriers thermally emitted out of the quantum well studied are captured and recombine in the neighboring thicker wells for which thermal emission does not occur until higher temperatures are reached. This physical picture is clearly supported by data shown in Figs. 5(b) and 6. With this assumption, the kink in the luminescence versus temperature plot corresponds to the temperature at which the rate of thermal emission (e_n^t) out of the quantum well is of similar magnitude as the recombination rate: $e_n^t \approx \tau_{\text{rec}}^{-1}$. If one can assume an average value of τ_{rec} for different temperatures and for different quantum-well widths,^{31,43,44} each such critical temperature T' should correspond to a fixed value of the thermal emission rate. Hence, by compiling data for T' and the corresponding activation energies for the thermal emission process, it should be possible to model emission and capture processes for quantum wells.

The critical temperatures are plotted in Fig. 8 (kT' in meV) versus the exciton binding energy which approximately equals the sum of the barrier energies of electrons and holes, $\Sigma E_b = E_g(\text{InP}) - h\nu(\text{QW})$, where $h\nu(\text{QW})$ is the energy of luminescence from the quantum well studied. It is quite clear that the data may be described by a straight line, indicating that the quantity $\Sigma E_b / (kT')$ is kept constant for all six values of ΣE_b , with the proportionality relation:

$$kT' = 0.053 \Sigma E_b . \quad (2)$$

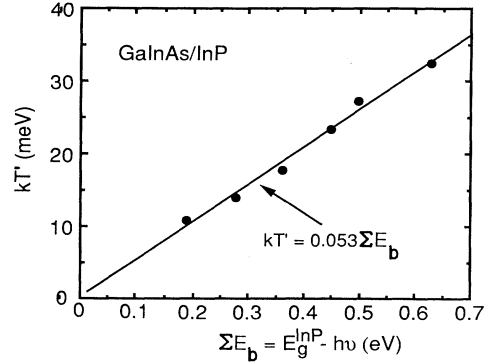


FIG. 8. A plot of the critical temperature (as kT') at which a kink in the curve of PL intensity vs temperature occurs, namely the onset of the quenching process, as a function of the sum of the barrier energies of electrons and holes. Best square fit to the data yields a straight line with a slope of 0.053.

In order to get a physical interpretation of the relationship found it is noted that, by the application of the principle of detailed balance, the rates for emission (e_n^t) and capture (c_n) are related as

$$e_n^t = c_n \exp(-\Delta E / kT) \quad (3a)$$

and for the critical temperature T' this detailed balance expression can be rewritten

$$\tau_{\text{rec}}^{-1} = e_n^t = c_n \exp(-\Delta E / kT') , \quad (3b)$$

where ΔE is the thermal activation energy (Gibbs free energy) for the emission process.

If the exciton emission case (i.e., $\Delta E = \Sigma E_b$) is evaluated quantitatively it can be deduced from Eq. (3b) that $\tau_{\text{cap}} = c_n^{-1} = \tau_{\text{rec}} \exp(-\Delta E / kT') \approx \tau_{\text{rec}} \exp(-1 / 0.053)$. With the estimation of $\tau_{\text{rec}} \approx 10$ ns,^{31,44} capture times shorter than fs are obtained. This is obviously an unrealistically fast capture time, which leads us to the conclusion that it is not the entire exciton which is emitted out of the QW at the onset of quenching but that it is, instead, the most weakly bound particle which determines when the QW excitonic recombination is thermally quenched.

The way that the total barrier for excitons is separated into the barrier for the electron and the hole can be estimated using the envelope-function approach for calculating energy states of QW's. It is found that for the series of QW's studied, the electron is the most weakly bound particle and that the portion of the total barrier height occurring as activation energy for the electron ranges from $\xi=0.25$ for ultrathin QW's to $\xi=0.40$ for thicker layers. Using the same approximation as above for the constant recombination time, the characteristic times for carrier capture into the quantum wells can hence be estimated as

$$\begin{aligned} \tau_{\text{cap}} &= c_n^{-1} = \tau_{\text{rec}} \exp(-\Delta E_{el} / kT) \\ &\approx \tau_{\text{rec}} \exp(-\xi / 0.053) , \end{aligned} \quad (4)$$

where $\xi = \Delta E_{el} / \Sigma E_b$ is the fraction of the total barrier energy, ΣE_b , which is playing the role of activation energy for the quenching process of the most weakly bound electron. If the value of $\xi \approx 0.25$ is used, i.e., $\Delta E = 0.25 \Sigma E_b$, this leads to the numerical evaluation of the carrier capture time into the quantum wells as $\tau_{cap} \approx \tau_{rec} 9 \times 10^{-3} \approx 100$ ps, assuming $\tau_{rec} \approx 10$ ns. For comparison, with the use of $\xi = 0.4$, it can be estimated that $\tau_{cap} \approx \tau_{rec} 5 \times 10^{-4} \approx 5$ ps. It is quite interesting to compare this range of capture times into quantum wells with the direct observation of barrier luminescence decay times from which Deveaud *et al.*⁴² have estimated τ_{cap} to be in the range of a few ps.

Obviously, the above evaluation of capture times into QW's has large errors since the actual recombination time at the temperature for which quenching starts is not known and since it can be expected to vary with temperature as well as with the thickness of the wells. Furthermore, the assumption that the carriers, which are emitted out of a QW, are not recaptured but instead captured into a neighboring, thicker QW, may lead to an overestimation of the emission time constant. In future work it is hoped that the careful design of multiple QW samples can reduce this uncertainty and also that the actual recombination times will be measured at the temperatures at which the PL is quenched due to the thermal emission.

D. Quantitative analysis of exciton migration, based on absorption and luminescence measurements

It is highly desirable to be able to get a quantitative understanding of the exciton dynamics discussed above. In order to attain this insight absorption measurements are performed. A special sample (EQ99) was grown, with ten identical QW's, each of a nominal thickness of 3 ML. In Fig. 9 absorption data through the stack of QW's are plotted. Spectra (a)–(g) are obtained from different spots on the sample wafer, the distance between two consecutive spectra being ≈ 3 mm. It is quite clear from Fig. 9 that the main absorption feature is an excitonic absorption peak at approximately 1.19 eV. In the bottom two spectra, which are obtained from the part of the wafer with the higher growth rate, the exciton absorption peak of 1-ML thicker regions are also seen, with the excitonic absorption peak at approximately 1.14 eV. The structures seen at higher energy are believed to be due to light-hole absorption peaks and will not be discussed further. Assuming that the optical transition probability is the same for QW's with ± 1 ML thickness, the relative strengths of the QW excitonic absorption peaks should reflect directly the areas of monolayer islands within the QW studied. Distortion of absorption spectra due to band filling is not expected for the low levels of doping in the samples studied here.

Figure 10 shows the PL spectra obtained from the same seven spots at which the absorption spectra in Fig. 9 were taken. These data were collected on the same occasion with the sample at a temperature of 5 K. The same trend between the different spots is seen in PL intensity, but with the difference that the low-energy peaks

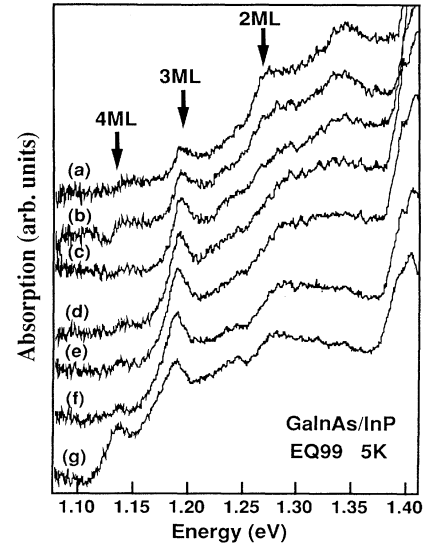


FIG. 9. Absorption spectra of sample EQ99 at 5 K. The sample contains ten QW's with nominally identical thickness. Spectra (a)–(g) correspond to different positions on the sample along a direction of increasing growth rate. The relative intensity of different absorption peaks reflects the relative areas of monolayer islands.

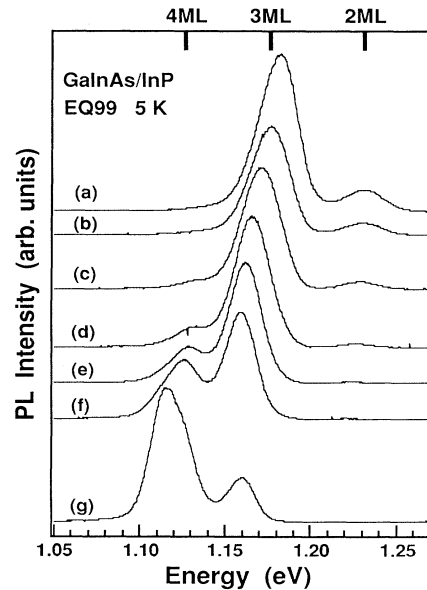


FIG. 10. Photoluminescence spectra of sample EQ99 at 5 K. Spectra (a)–(g) are taken at the same spot on the sample as the positions (a)–(g) in Fig. 9. Comparing the results obtained from the same sample position, the relative intensity of peaks is different in the PL spectra in the figure and the absorption spectra in Fig. 9. Due to significant exciton migration exists even at 5 K; attempts to estimate the relative areas of monolayer islands from PL intensities lead to an overestimation of the area of thicker islands.

are always overrepresented due to transfer and thermalization processes. As an example, the bottom PL spectrum [curve (g)] shows the PL intensity of the 4-ML islands as ≈ 3 times that of the 3-ML islands, $I_{4\text{ML}}:I_{3\text{ML}} \approx 3:1$, while in the absorption spectrum, surprisingly one gets $I_{4\text{ML}}:I_{3\text{ML}} \approx 1:2$. Therefore, if one tries to estimate the ratio of areas of islands of different thicknesses from low-temperature PL intensity, he will greatly overestimate the area of thicker islands. This agrees with the conclusion drawn in Sec. III B 3 where island areas are determined from high-temperature PL intensity.

An attempt can be made to quantitatively determine the amount of down-hill exciton transfer at low temperatures. From the absorption measurement at position (g) in Fig. 9, $S_{4\text{ML}}:S_{3\text{ML}} \approx 1:2$, while the low-temperature PL at the same position shows relative intensities of $I_{4\text{ML}}:I_{3\text{ML}} \approx 3:1$. Hence 1.25 of the two units will have transferred at 5 K, resulting in a relative PL intensity of $(1 + 1.25)/(2 - 1.25) = \frac{3}{1}$. This comparison suggests that even at 5 K the excitons will not be completely localized but that more than 60% of the areas of the thinner QW's excitons will still diffuse to the border of the 4-ML island regions and recombine there. A topological explanation of this analysis may be that closer to the rim of the regions of the thinner QW, excitons may find, in two dimensions, routes which will bring them to the border without having to overcome energetic barriers. Such connecting paths are expected to occur and the mathematics of this problem of topology is quite interesting. Still, some of the excitons captured into the thinner well regions are truly localized by potential fluctuations which are not connected to the intrawell QW borders.

The analysis performed in this section shows semiquantitatively how the areas, as determined by absorption spectroscopy, markedly differ from those estimated from PL data. The results suggest a reevaluation of the results of CL image studies reported in the literature, since the CL images of monolayer flat islands in a QW will obviously depend on temperature. Even at the lowest temperature, since the exciton migration is nevertheless significant, the thicker islands will appear to be larger than the real area of the island. Furthermore, in the temperature region of thermally activated, down-hill migration, one would expect to observe an apparent expansion of thicker islands with increasing temperature, with a simultaneous shrinkage of the thinner islands. Of course, this is true provided that the size of monolayer islands is greater than the diffusion length of excitons. Otherwise, exciton migration probably affects only the contrast, but not the topological appearance of the CL images.

E. Phenomena associated with different samples

In general, all the four exciton dynamics: (α) localization, (β) down-hill migration, (γ) up-hill thermalization, and (δ) interwell capture and emission, are observed in our different samples. The typical temperature at which a particular process starts to dominate the exciton dynamics, however, can vary from sample to sample. This is not difficult to understand since each process has its

characteristic activation energy. The activation energy for process δ is determined by the carrier confinement energy which depends on the QW thickness. The activation energy for up-hill thermalization is related to the difference in the exciton confinement energies of QW's with thicknesses differing by one monolayer. The thermally activated, down-hill migration, however, should be determined by the localization potential.

Already for the two samples investigated in this study, EQ72 and EQ99, such sample-dependent characteristic temperatures are observed. Figure 11 shows temperature-dependent PL spectra for EQ99 at a sample position close to position (c), as discussed in Sec. III D. Processes α , β , and γ are readily observed, while process δ is indicated as a decrease in overall intensity since the sample contains a stack of ten QW's of equal thickness. From a comparison between the behavior of this sample and that shown in Figs. 5 and 6 it is seen that the thermally activated exciton migration starts at a higher temperature for EQ99 than for EQ72. In EQ99 (Fig. 11) the PL intensity remains almost constant up to 40 K (the temperature range of exciton localization), while in EQ72 (Fig. 6) the process of thermally activated, down-hill migration dominates in the temperature range between 10 and 45 K. The reason for the difference in behavior may be attributed to the differences in the size of islands

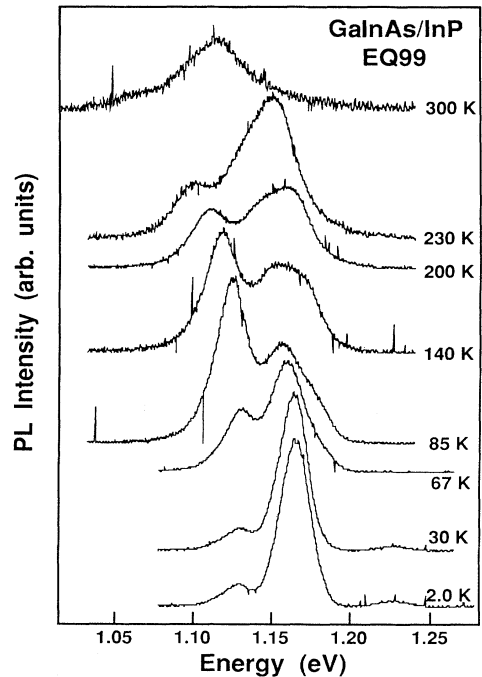


FIG. 11. Temperature-dependent, photoluminescence spectra of EQ99 at a sample position close to (d) in Fig. 10. Different exciton dynamics similar to those discussed in Figs. 5 and 6 for sample EQ72 are readily observed. The main difference between the behavior of these two samples lies in the lowest temperature at which the thermally activated, down-hill migration starts. For sample EQ72 this temperature is observed to be about 10 K, while for sample EQ99 it is more than 40 K.

and/or the magnitude of potential fluctuations in the QW. In fact the growth procedures are different for samples EQ72 and EQ99, and sample EQ99 was grown more than one year later in a slightly different growth system.

In this connection, it should be pointed out that in a recently published paper, Bacher *et al.* reported similar phenomena in their $\text{Ga}_{0.47}\text{In}_{0.53}\text{As}/\text{InP}$ quantum wells.³¹ Their samples turned out to be more similar to our sample EQ99 than EQ72, since a fairly high temperature for the activation of the down-hill exciton migration was observed. However, the most significant difference in the conclusion drawn from their studies and our present study lies in the temperature region of exciton localization. According to their conclusion, exciton localization dominates at low temperatures. That no transfer exists at 13 K in their sample was supported by the time-resolved PL spectra between 175 and 3700 ps. This is contrary to our conclusion drawn from both high-temperature PL and absorption studies, that even at the lowest temperature, significant transfer of excitons occurs, in spite of a temperature-independent PL intensity. It seems that the transfer process has no potential barrier and is not temperature activated. If our conclusion is universal, and since this transfer was not observed after a time delay of 175 ps in their sample, then such a low-temperature transfer should probably be very fast—faster than in the region of a few hundred ps.

Before we summarize, it is worth noting that in some other samples, the existence of extended, almost-monolayer flat islands is also observed as “monolayer splitting” in the luminescence spectra, and a discontinuous shift of luminescence peaks to lower energies along the direction of higher growth rates on the sample. However, the energy separation between the peaks of monolayer splitting varies as the laser spot is scanned over the sample.⁴⁵ The variation can be as much as 20 meV, indicating that interface islands are not really atomically smooth. A modified picture of monolayer flat islands should probably be introduced, in which microroughnesses on a scale of lengths shorter than the exciton diameter, is superimposed on extended, monolayer flat islands. In fact, in the PL spectra in Fig. 10 a strong variation in the peak position (> 20 meV) is seen while the position of the peak energy in absorption (Fig. 9)

remains almost constant (< 5 meV). From this comparison one can determine that the PL shift is not related to variation in alloy composition but rather is due to spatial variation in the tail of the density of state, related to interface microroughness.

In summary, spectroscopic studies have been performed on multiple-quantum-well structures of lattice-matched $\text{Ga}_{0.47}\text{In}_{0.53}\text{As}/\text{InP}$. The structures are grown by low-pressure, metal-organic vapor-phase epitaxy. The compositional gradient and thickness variation at interfaces are probed by exciton recombination in the quantum wells. Spectral and topological observations of extended, monolayer flat islands are demonstrated by photoluminescence and cathodoluminescence. The features of the temperature-dependent photoluminescence spectra of the quantum wells are explained in terms of different exciton transfer mechanisms dominating in different temperature regions: (α), localization at the low temperatures; (β), down-hill migration; (γ), up-hill thermalization at intermediate temperatures; and (δ), interwell emission; and capture at high temperatures. Furthermore, from the high-temperature, thermal quenching of the luminescence, ps-fast time constants have been estimated for carrier capture into quantum wells. Finally, absorption measurement is proposed and employed to determine the ratio of the area of monolayer islands in a quantum well. From a comparison between absorption and luminescence results, conclusions are drawn that low-temperature luminescence intensity greatly overestimates the area of thicker islands, which, among other things, calls for a reevaluation of the results concerning the image of extended, monolayer flat islands by cathodoluminescence.

ACKNOWLEDGMENTS

The authors are grateful to Dr. M.-E. Pistol for fruitful discussions; to Dr. A. Gustafsson for assistance in CL measurements; to Dr. G. Wagner, Leipzig for assistance in HRTEM measurements; and to Epiquip AB for the growth of the samples. This work was supported by the Swedish Natural Science Research Council (NFR) and the Swedish National Board for Industrial and Technical Development (NUTEK).

*Present address: Hearst Mining Building, Department of Materials Science, University of California at Berkeley, Berkeley, CA 94720.

†Present address: Institut für Halbleiterphysik, D-(O)-1200 Frankfurt/Oder, Federal Republic of Germany.

¹Application of *Multiquantum Wells, Selective Doping, and Superlattices*, edited by R. K. Willardson and A. C. Beer, Semiconductors and Semimetals Vol. 24 (Academic, San Diego, 1987).

²C. Weisbuch and B. Vinter, in *Quantum Semiconductor Structures* (Academic, Boston, 1991).

³T. Sakamoto, H. Funabashi, K. Ohta, T. Nakagawa, N. J. Kawai, T. Kojima, and K. Bando, *Superlatt. Microstruct.* **1**, 347 (1985).

⁴B. A. Joyce, P. J. Dobson, J. H. Neave, K. Woodbridge, J. Zhang, P. K. Larsen, and B. Bölger, *Surf. Sci.* **168**, 423 (1986).

⁵W. T. Tsang and E. F. Schubert, *Appl. Phys. Lett.* **49**, 220 (1986).

⁶W. T. Tsang, T. H. Chiu, J. E. Cunningham, and A. Robertson, *Appl. Phys. Lett.* **50**, 1376 (1987).

⁷K. Ploog, *J. Cryst. Growth* **79**, 887 (1986).

⁸D. E. Aspnes, R. Bhat, E. Colas, V. G. Keramidis, M. A. Koza, and A. A. Studna, *J. Vac. Sci. Technol. A* **7**, 711 (1989).

⁹D. Grützmacher, J. Hergeth, F. Reinhardt, K. Wolter, and P. Balk, *J. Electron. Mater.* **19**, 471 (1990).

¹⁰T. Fukunaga, K. L. I. Kobayashi, and H. Nakashima, *Jpn. J. Appl. Phys.* **24**, L510 (1985).

¹¹M. Tanaka and H. Sakaki, *J. Cryst. Growth* **81**, 153 (1987).

¹²T. Y. Wang, K. L. Fry, A. Persson, E. H. Reihlen, and G. B. Stringfellow, *Appl. Phys. Lett.* **52**, 290 (1988).

¹³P. M. Petroff, J. Cibert, A. C. Gossard, G. J. Dolan, and C. W. Tu, *J. Vac. Sci. Technol. B* **5**, 1204 (1987).

- ¹⁴D. Bimberg, J. Christen, T. Fukunaga, H. Nakashima, D. E. Mars and J. N. Miller, *J. Vac. Sci. Technol. B* **5**, 1191 (1987).
- ¹⁵M. Irikawa, I. J. Murgatroyd, T. Ijichi, N. Matsumoto, A. Nakai, and S. Kashiwa, *J. Cryst. Growth* **93**, 370 (1988).
- ¹⁶M. Kondo, S. Yamazaki, M. Sugawara, H. Okuda, K. Kato, and K. Nakajima, *J. Cryst. Growth* **93**, 376 (1988).
- ¹⁷W. Seifert, J.-O. Fornell, L. Ledebø, M.-E. Pistol, and L. Samuelson, *Appl. Phys. Lett.* **56**, 1128 (1990).
- ¹⁸C. Weisbuch, R. C. Miller, R. Dingle, A. C. Gossard, and W. Wiegmann, *Solid State Commun.* **37**, 219 (1981). C. Weisbuch, R. Dingle, A. C. Gossard, and W. Wiegmann, *ibid.* **38**, 709 (1981).
- ¹⁹D. Grützmacher, *J. Cryst. Growth* **107**, 520 (1991).
- ²⁰O. Albrektsen, D. J. Arent, H. P. Meier, and H. W. M. Salemink, *Appl. Phys. Lett.* **57**, 31 (1990).
- ²¹A. Ourmazd, D. W. Taylor, J. Cunningham, and C. W. Tu, *Phys. Rev. Lett.* **62**, 933 (1989).
- ²²M. A. Herman, D. Bimberg, and J. Christen, *J. Appl. Phys.* **70**, R1 (1991), and references therein.
- ²³J. Singh, K. K. Bajaj, and S. Chaudhuri, *Appl. Phys. Lett.* **44**, 805 (1984).
- ²⁴G. Bastard, C. Delalande, M. H. Meynadier, P. M. Frijlink, and M. Voos, *Phys. Rev. B* **29**, 7049 (1984). C. Delalande, M. H. Meynadier, and M. Voos, *ibid.* **31**, 2497 (1985).
- ²⁵B. Deveaud, T. C. Damen, J. Shah, and C. W. Tu, *Appl. Phys. Lett.* **51**, 828 (1987).
- ²⁶D. S. Jiang, H. Jung, and K. Ploog, *J. Appl. Phys.* **64**, 1371 (1988).
- ²⁷K. Fujiwara, K. Knamoto, and N. Tsukada, *Phys. Rev. B* **40**, 9698 (1989).
- ²⁸M. Kohl, D. Heitmann, S. Tarucha, K. Leo, and K. Ploog, *Phys. Rev. B* **39**, 7736 (1989).
- ²⁹T. Takagahara, *J. Lumin.* **44**, 347 (1989).
- ³⁰L. Samuelson, X. Liu, and S. Nilsson, in *Proceedings of the 20th International Conference on the Physics of Semiconductors*, edited by E. M. Anastassakis and J. D. Joannopoulos (World Scientific, Thessaloniki, 1990), p. 1625.
- ³¹G. Bacher, J. Kovac, K. Streubel, H. Schweizer, and F. Scholz, *Phys. Rev. B* **45**, 9136 (1992).
- ³²A. Gustafsson, J. Jönsson, M. Gerling, M. R. Leys, M.-E. Pistol, L. Samuelson, and H. Titze, in *Microscopy of Semiconducting Materials*, edited by A. G. Cullis and J. L. Hutchison, IOP Conf. Proc. No. 100 (Institute of Physics and Physical Society, London, 1989), p. 771.
- ³³B. G. Yacobi and D. B. Holt, in *Cathodoluminescence Microscopy of Inorganic Solids* (Plenum, New York, 1990).
- ³⁴K. W. Carey, R. Hull, J. E. Fouquet, F. G. Kellert, and G. R. Trott, *Appl. Phys. Lett.* **51**, 910 (1987).
- ³⁵J. Camassel, J. P. Laurenti, S. Juillaguet, F. Reinhardt, K. Wolter, H. Kurz, and D. Grützmacher, *J. Cryst. Growth* **107**, 543 (1991).
- ³⁶H. Kamei and H. Hayashi, *J. Cryst. Growth* **107**, 567 (1991).
- ³⁷G. Landgren, P. Ojala, and O. Ekström, *J. Cryst. Growth* **107**, 573 (1991).
- ³⁸K. Streubel, V. Härle, F. Scholz, M. Bode, and M. Grundmann, *J. Appl. Phys.* **71**, 3300 (1992).
- ³⁹W. Seifert, K. Deppert, J. O. Fornell, X. Liu, S. Nilsson, M. E. Pistol, and L. Samuelson, *J. Cryst. Growth* (to be published).
- ⁴⁰S. Nilsson, A. Gustafsson, and L. Samuelson, *Appl. Phys. Lett.* **57**, 878 (1990).
- ⁴¹E. H. Reihlen, A. Persson, T. Y. Wang, K. L. Fry, and G. B. Stringfellow, *J. Appl. Phys.* **66**, 5554 (1989).
- ⁴²B. Deveaud, in *Proceedings of the 20th International Conference on the Physics of Semiconductors* (Ref. 30), p. 1021, and references therein.
- ⁴³R. Sauer, S. Nilsson, P. Roentgen, W. Heuberger, V. Graf, and A. Hangleiter, in *Proceedings of the 20th International Conference on the Physics of Semiconductors* (Ref. 30), p. 1133.
- ⁴⁴J. Feldmann, G. Peter, E. O. Göbel, P. Dawson, K. Moore, C. Foxon, and R. J. Elliott, *Phys. Rev. Lett.* **59**, 2337 (1987).
- ⁴⁵X. Liu, Ph. D. thesis, Lund University, Sweden, 1991.

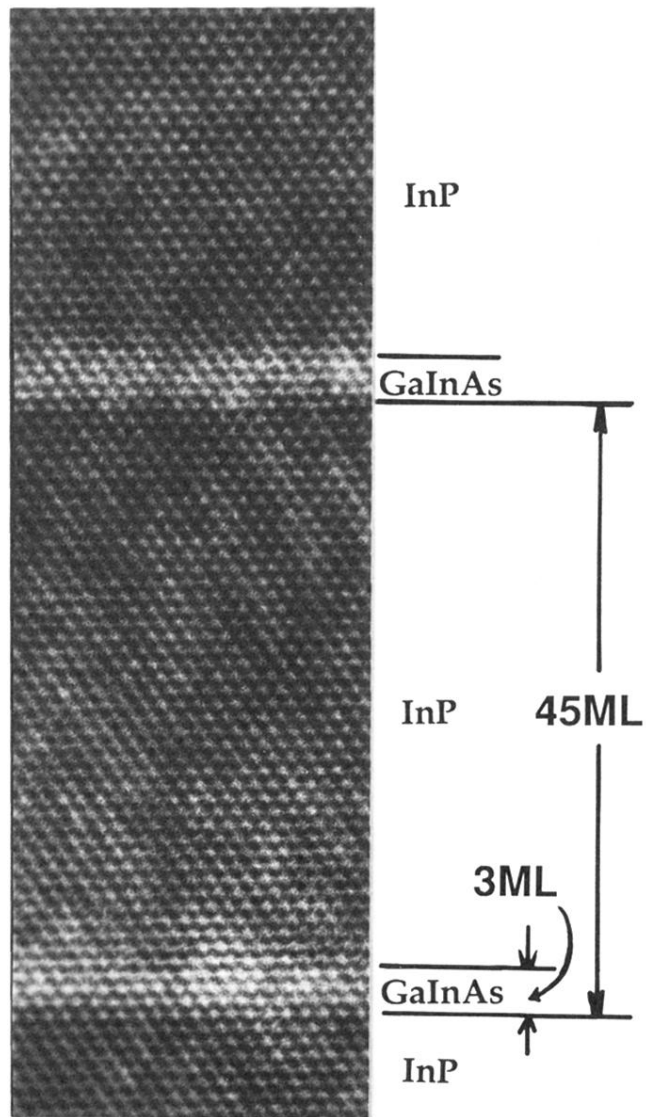


FIG. 2. Micrograph of $\text{Ga}_{0.47}\text{In}_{0.53}\text{As}/\text{InP}$ multiple-QW structures (sample EQ99) obtained from high-resolution transmission electron microscopy. It shows a sharp lower $\text{InP}/\text{Ga}_{0.47}\text{In}_{0.53}\text{As}$ interface and a more diffuse upper $\text{Ga}_{0.47}\text{In}_{0.53}\text{As}/\text{InP}$ interface. The exact thickness of the $\text{Ga}_{0.47}\text{In}_{0.53}\text{As}$ well is thus hard to determine. However, one can obtain a more accurate value of 45 ML for the thickness between two sharp interfaces, i.e., the thickness of the InP barrier plus the $\text{Ga}_{0.47}\text{In}_{0.53}\text{As}$ well. Taking into account the growth time of 3 min for the InP barrier and 6 s for the $\text{Ga}_{0.47}\text{In}_{0.53}\text{As}$ well, the thickness of the $\text{Ga}_{0.47}\text{In}_{0.53}\text{As}$ well can then be determined to be 3 ML.